

Cryogenic microjet for exploration of superfluidity in highly supercooled molecular hydrogen

R. E. GRISENTI¹, R. A. COSTA FRAGA¹, N. PETRIDIS¹, R. DÖRNER¹ and J. DEPPE²

¹ *Institut für Kernphysik, J. W. Goethe Universität*

Max-von-Laue-Str. 1, 60438 Frankfurt (M), Germany

² *LaVision GmbH - Anna-Vandenhoeck-Ring 19, 37081 Göttingen, Germany*

received 2 November 2005; accepted in final form 21 December 2005

published online 11 January 2006

PACS. 47.27.Wg – Jets.

PACS. 39.10.+j – Atomic and molecular beam sources and techniques.

PACS. 47.27.Te – Convection and heat transfer.

Abstract. – We describe a new approach to producing a sample of supercooled molecular para-hydrogen ($p\text{H}_2$) at temperatures down to 1.3 K, well below the predicted superfluid transition temperature for $p\text{H}_2$. Unique features of the present scheme are 1) the suppression of both homogeneous and heterogeneous nucleation processes and 2) the possibility to control the liquid temperature in a wide range across the transition. As a first step we demonstrate the stable production in vacuum of continuous hydrogen filaments of macroscopic dimensions. This technique coupled to light scattering experiments will enable microscopic investigations of superfluidity in liquid para-hydrogen.

Superfluids are unique among all materials. Properties such as the absence of viscosity, the possibility to flow through narrow channels that are practically impermeable to conventional liquids, or the virtually infinite thermal conductivity make superfluidity one of the most peculiar and counterintuitive of all phenomena [1]. Superfluid liquids are, however, rare: the only known examples are the helium liquids ^4He and ^3He . The next most natural candidate for superfluidity appears to be liquid molecular hydrogen in the nuclear spin configuration $I = 0$ called para-hydrogen. At low temperatures, $p\text{H}_2$ is in the ground rotational state $J = 0$ and thus, like ^4He , is a spinless boson. Ginzburg and Sobyenin in 1972 [2] were apparently the first to discuss the possibility of Bose-Einstein condensation (BEC) and superfluidity in bulk liquid para-hydrogen. They concluded that $p\text{H}_2$ might undergo a superfluid transition at about 6.6 K. More recent calculations predict a lower transition temperature of $T_c = 2\text{--}3\text{ K}$ [3–5]. However, with its triple-point at 13.8 K $p\text{H}_2$ is already a solid at the temperature at which BEC is predicted to occur. This is a major obstacle in an effort to observing superfluidity in bulk $p\text{H}_2$. A superfluid transition temperature far below the triple point requires extensive supercooling, and maintaining the liquid state at such low temperatures for a sufficiently long time to enable the exploration of superfluidity represents a challenging experimental task. Indeed, several ingenious experimental approaches have all failed over the last 20 years in achieving the required supercooling (see [6–8] and references therein). The only indirect experimental evidence

that $p\text{H}_2$ can indeed become superfluid comes from high-resolution infrared spectroscopy of OCS-doped $p\text{H}_2$ clusters with up to 17 molecules, which are inside ultra-cold helium clusters produced in free-jet expansions into vacuum [9]. These results provide evidence for a new superfluid state of matter defined so far only in the nanoscale regime, where the problem of supercooling has been circumvented by significantly reducing the molecular density.

Here we describe a novel simple method for the experimental realization of a target of supercooled bulk molecular para-hydrogen at temperatures below T_c . Our approach is based on liquid microjet generation by forcing $p\text{H}_2$ at cryogenic source conditions (pressure P_0 and temperature T_0) through a pinhole orifice into vacuum. Under laminar flow conditions (for Reynold's numbers $\text{Re} \lesssim 1200$, with $\text{Re} = \rho v d_0 / \eta$, where ρ is the density of the liquid, η is the coefficient of viscosity, d_0 is the orifice diameter, and v is the flow velocity) the liquid propagates as a contiguous cylindrical filament until it spontaneously breaks up into a monodirectional stream of droplets [10]. The contiguous filament provides a *well-defined, boundary-free sample of macroscopic dimensions* that virtually *enables indefinite observation time*. On that account continuous laminar liquid jets have found in recent years widespread applications. Water microjets as introduced by Faubel *et al.* [11] opened up new ways for photoelectron spectroscopy [12] and X-ray absorption spectrometry [13]. Liquid microjets are also used as targets for laser-induced production of debris-free X-ray and EUV sources [14]. The above experiments strongly benefit from the clean, continuously replenished liquid surface as provided by a laminar liquid jet propagating in a vacuum region. It is anticipated here that for liquid hydrogen this unique feature would greatly suppress the severe problem of heterogeneous nucleation via surface contamination. The aim of the present letter is thus to demonstrate that for a para-hydrogen microjet a filament temperature as low as 1.3 K *can be achieved* upstream of jet breakup.

The classical theory on the instability and disintegration of an inviscid liquid jet discharged into vacuum was first given in the late 1800s by Rayleigh, whose name it now bears [15]. The orifice (or “nozzle”) diameter d_0 sets the length scale for all the critical dimensions of the flow, including the droplet diameter after breakup, $1.9d_0$, and the length ℓ of the contiguous filament from the nozzle exit to the breakup point, $\ell \simeq 12v(\rho d_0^3 / \sigma)^{1/2}$ for fluids of low viscosity, where σ is the surface tension of the liquid. Recent experiments with normal liquid and superfluid helium microjets [16] indicated that for a thin walled orifice the jet velocity is related to the source pressure by the Bernoulli equation $v = \sqrt{2P_0/\rho}$. The low viscosity of liquid hydrogen limits the nozzle diameter for stable laminar flow to $d_0 < 3 \mu\text{m}$ with P_0 in the range $P_0 = 1\text{--}10$ bar.

As the liquid jet expands into vacuum it evaporatively cools. Following Faubel *et al.* [11] we have computed the continuous jet axial temperature profile $T(z)$ for the case of simple evaporative cooling for a 2 μm -dia. nozzle and for source conditions $P_0 = 8$ bar and $T_0 = 16$ K. The result is shown in fig. 1 by the dotted line. It can be seen that the lowest liquid $p\text{H}_2$ stream temperature of ≈ 8 K near breakup is still much higher than T_c . Evaporative cooling is intrinsically constrained by the exponential drop in vapor pressure of the liquid with decreasing temperature. Conduction and convection of thermal energy from the ambient gas to the liquid can, however, strongly alter the cooling process. In particular, by choosing appropriately the species and temperature of the ambient gas, one may *enhance cooling* of the liquid stream. The obvious choice is represented by helium gas at temperatures $< T_c$. Of the two helium isotopes, ^3He appears to be better suited for the present purposes because of 1) the larger thermal conductivity and 2) the higher saturated vapor pressure at temperatures below 2 K [17]. From the practical point of view, the helium gas would be partially enclosed at a set pressure P_{He} in a copper cell centered about the jet flight path and attached to a He bath cryostat providing temperatures from 4 K down to 1.3 K [16]. We will show that ambient pressures as low as $P_{\text{He}} \sim 10^{-2}$ bar [18] are adequate to attain filament temperatures below T_c .

The heat transfer process is described by the energy balance equation $V\rho c_p dT = \rho L dV + Ah(T_{\text{He}} - T)dt$, where $c_p(T)$ is the heat capacity of the liquid, L is the heat of evaporation, h is the heat transfer coefficient, and T_{He} is the helium gas temperature. For the specific case of a cylindrical geometry the surface area A and the volume V are expressed per unit length. From the definition $v = dz/dt$ there follows

$$r \frac{dT}{dz} = \frac{2L}{c_p(T)} \frac{dr}{dz} + \frac{2h(T_{\text{He}} - T)}{\rho v c_p(T)}, \quad (1)$$

where $r(z)$ is the filament radius. The overall heat transfer coefficient is defined as $h = (\kappa_{\text{He}}/2r)\text{Nu}$, where κ_{He} is the ambient gas thermal conductivity. The definition of the Nusselt number Nu depends on the actual flow regime as expressed by Reynold's number $\text{Re}_{\text{He}} = (2r\rho_{\text{He}}/\eta_{\text{He}})v$, where $\rho_{\text{He}} \propto P_{\text{He}}/T_{\text{He}}$ and η_{He} are the density and the coefficient of viscosity of the helium gas, respectively. Under the ambient gas conditions of interest here ($P_{\text{He}} \sim 10^{-2}$ bar, $T_{\text{He}} \leq 3$ K) $\rho_{\text{He}} \sim 10^{-3}$ g/cm³ and $\eta_{\text{He}} \sim 10^{-5}$ poise [17]. Thus $\text{Re}_{\text{He}} \sim 10^2$ ($v \sim 10^2$ m/s) and the resulting flow is laminar. In this case Nu is conveniently expressed by the Ranz-Marshall correlation [19] $\text{Nu} = 2 + 0.6\text{Re}_{\text{He}}^{1/2}\text{Pr}_{\text{He}}^{1/3}$, with $\text{Pr}_{\text{He}} = c_{p,\text{He}}\eta_{\text{He}}/\kappa_{\text{He}}$, where $c_{p,\text{He}}$ is the ambient gas heat capacity.

In the presence of the ambient gas the mass transfer process is best described by a diffusion-controlled model, $dN = -\gamma A(n_{\text{sat}} - n_{\infty})dt$, where n_{sat} and n_{∞} are the concentrations of the vapor molecules near the filament surface (and assumed to coincide with that at saturation) and at infinity, respectively. The mass transfer coefficient is defined as $\gamma = (D/2r)\text{Sh}$, where D is the diffusion constant and the Sherwood number for mass transfer correlation is given by $\text{Sh} = 2 + 0.6\text{Re}_{\text{He}}^{1/2}\text{Sc}_{\text{He}}^{1/3}$, where $\text{Sc}_{\text{He}} = \eta_{\text{He}}/(D\rho_{\text{He}})$ [19]. The partial hydrogen concentration n_{∞} is an unknown experimental parameter; however, we may approximate $n_{\infty} \approx 0$ by noting that most of the evaporated hydrogen molecules would condense on the walls of the cell containing the helium gas, kept at $T_{\text{He}} < 4$ K. The mass loss equation takes thus the form

$$\frac{dr}{dz} = -\frac{\gamma m}{\rho v} \frac{p_{\text{sat}}(T)}{kT}. \quad (2)$$

For the temperature range considered here the liquid density and the heat of evaporation have been assumed to be constant, whereas for the heat capacity an extrapolation to low temperatures of the linear dependence shown by Andreev has been used [3]. For the saturation vapor pressure in eq. (2) we have assumed the temperature dependence reported in [20].

The liquid filament temperature $T(z)$ computed according to eqs. (1) and (2) with the boundary conditions $T(0) \equiv T_0 = 16$ K and $2r(0) \equiv d_0 = 2$ μm and for $P_0 = 8$ bar is plotted in fig. 1. The solid line is for ³He gas at $P_{\text{He}} = 3.5 \cdot 10^{-2}$ bar and $T_{\text{He}} = 1.3$ K. One can see that forced cooling yields a final continuous liquid pH₂ stream temperature of $T \approx 1.3$ K, which is *well below* the predicted superfluid transition temperature T_c . This reflects a cooling rate $> 10^6$ K/s for $z \lesssim 0.6$ mm, up to one order of magnitude larger than for the case of simple evaporative cooling, as shown in the inset of fig. 1. The assumed P_{He} is close to the saturated ³He vapor pressure at 1.3 K. The effect of a higher P_{He} is shown by the dashed curve in fig. 1, which corresponds to the calculated $T(z)$ during interaction with ³He gas at $P_{\text{He}} = 6.5 \cdot 10^{-2}$ bar and $T_{\text{He}} = 1.5$ K. The continuous liquid stream rapidly cools to a final temperature close to that of the gas, and beyond a distance of ≈ 0.6 mm from the nozzle exit the temperature only slightly further decreases up to the breakup point. A nearly constant filament temperature over a macroscopic length greater than 0.2 mm is important to compensate for finite thermal diffusion effects. The characteristic time needed to achieve a uniform radial filament temperature is $\tau_T \approx d_0^2/(4D_T)$, where $D_T(T) = \kappa_T(T)/[c_p(T)\rho]$

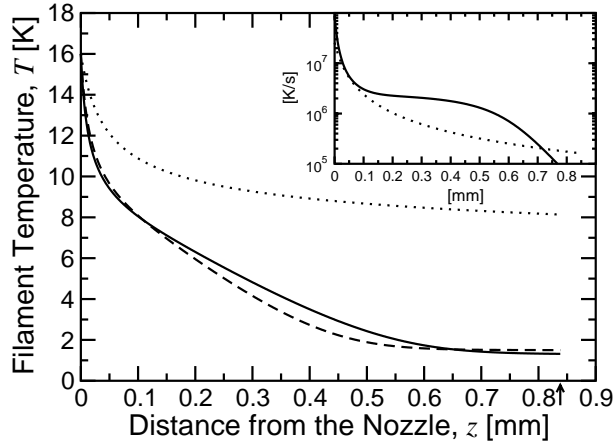


Fig. 1 – Axial filament temperature profiles calculated for the case of simple evaporative cooling [11] (dotted line) and via *forced cooling* according to eqs. (1) and (2) for $P_{\text{He}} = 3.5 \cdot 10^{-2}$ bar and $T_{\text{He}} = 1.3$ K (solid line), and $P_{\text{He}} = 6.5 \cdot 10^{-2}$ bar and $T_{\text{He}} = 1.5$ K (dashed line). The source parameters are $d_0 = 2 \mu\text{m}$, $P_0 = 8$ bar and $T_0 = 16$ K. The corresponding flow velocity and filament length are $v \simeq 145$ m/s and $\ell \simeq 0.84$ mm (indicated by the arrow), respectively. The inset shows the calculated cooling rates, where the lines have the same meaning explained above.

is the thermal diffusivity of the liquid, being $\kappa_T(T)$ the liquid thermal conductivity [6]. At temperatures below 4 K is $\tau_T < 1 \mu\text{s}$, corresponding to a flight path $v\tau_T < 0.15$ mm.

Throughout the above discussion we assumed implicitly that the liquid stream remains in a metastable liquid state. Indeed, it turns out that solidification via homogeneous nucleation is *greatly suppressed* by the combination of short flight times and high cooling rates demonstrated here. Theoretical investigations of the nucleation process in $p\text{H}_2$ indicated that the homogeneous nucleation rate $\Gamma(T)$ has a maximum Γ_{max} , $10^{12} \lesssim \Gamma_{\text{max}} \lesssim 10^{16} \text{ cm}^{-3}\text{s}^{-1}$, at $T_{\text{max}} \approx 7$ K [3, 21]. Accordingly, if τ is the time for the liquid stream to cool through the temperature range near Γ_{max} , to avoid freezing one needs $V\tau\Gamma_{\text{max}} < 1$ [6]. By assuming a cylindrical volume element equal to the droplet volume after Rayleigh breakup, $V \approx 4d_0^3$, for the worse scenario with $\Gamma_{\text{max}} \approx 10^{16} \text{ cm}^{-3}\text{s}^{-1}$ we find $\tau < \tau_{\text{max}} \approx 3 \mu\text{s}$ for $d_0 = 2 \mu\text{m}$. Since during τ_{max} the liquid filament cools from T_0 to $T \approx 3$ K (see fig. 1), it follows that the above condition is satisfied by about one order of magnitude.

Crucial to the exploration of superfluidity in $p\text{H}_2$ with the method described above is the generation of a hydrogen microjet with diameter $d_0 \leq 2 \mu\text{m}$. However, the feasibility to producing stable continuous hydrogen filaments with the required dimension has yet to be demonstrated. We thus investigated liquid-hydrogen microjet generation in *vacuum* by means of high-resolution shadow imaging. Liquid normal hydrogen ($n\text{H}_2$) at source pressures $P_0 = 2\text{--}8$ bar and temperatures $T_0 = 15\text{--}18$ K was discharged through a $2 \mu\text{m}$ -dia. circular thin walled orifice (see fig. 2(a)) into a vacuum chamber pumped by a 2000 l/s turbo pump providing a pressure $\sim 10^{-5}$ mbar with the beam on. For the experiments with para-hydrogen a catalytic converter providing about 99% $p\text{H}_2$ concentration shall be needed [22]. The ultra-pure (99.9999%) $n\text{H}_2$ gas was liquified by means of a continuous-flow helium cryostat providing a temperature stabilization better than 5 mK. Shadow imaging of the jet was obtained with a 2048×2048 pixels resolution CCD camera allowing dual-frame operation mode at a minimum inter-frame time of < 150 ns. A double pulse Nd : YAG laser operating at 532 nm with a pulse width of less than 20 ns was used, coupled to a diffuser, for microjet backside illumination.

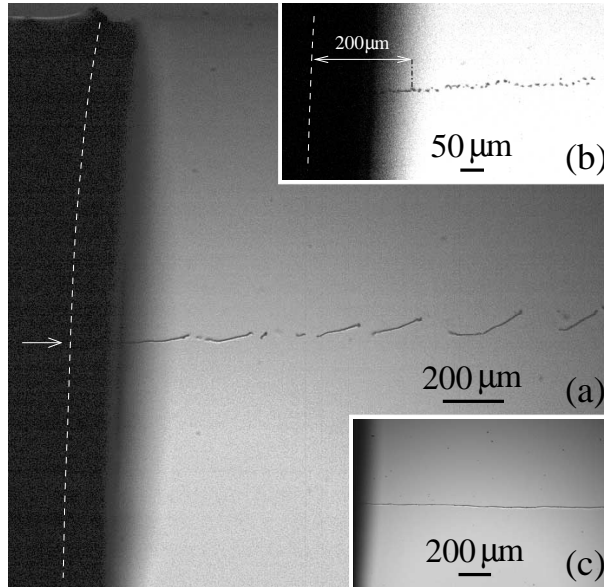


Fig. 2 – (a) Normal hydrogen microjet observed at $P_0 = 3$ bar and $T_0 = 16$ K showing breakup of the initial filament into a sequence of rods. The jet velocity is $v \approx 75$ m/s. The nozzle plate, visible on the left side, consists of a 2 mm-dia. and $\approx 3 \mu\text{m}$ thin circular foil (dashed line) containing the nominally $2 \mu\text{m}$ -dia. orifice (indicated by the arrow) and stuck on a $130 \mu\text{m}$ thick outer ring. (b) Close-up view of Rayleigh breakup observed at $P_0 = 4$ bar and $T_0 = 16$ K. The length of the continuous liquid filament is $\ell \approx 0.2$ mm. (c) Continuous solid filament observed at $P_0 = 3$ bar and $T_0 = 17$ K. As explained in the text, this represents the stable configuration for the $n\text{H}_2$ jet

Figure 2(a) shows the most frequent observation of microjet behavior, obtained at $P_0 = 3$ bar and $T_0 = 16$ K. It can be seen that at a distance of ≈ 0.4 mm from the nozzle exit the initial filament transforms into a sequence of long sections of jet material. The appearance of rods with a length up to $\approx 200 \mu\text{m}$ strongly suggests that the jet is already solid as breakup occurs. By comparing two successive frames separated by an inter-frame time of $1 \mu\text{s}$ it was possible to determine the velocity of the rods to be $v \approx 75$ m/s. This is only slightly below the velocity of 89 m/s predicted by the Bernoulli formula, indicating that the jet is liquid as it leaves the orifice. This was also confirmed (fig. 2(b)) by occasional observations of jet breakup characterized by the appearance of a sequence of micron-sized droplets as a result of Rayleigh oscillations inherent to *liquid* jets. The evidence for a contiguous filament length $\ell \approx 0.2$ mm (fig. 2(b)) about 50% shorter than expected is explained by external disturbances, *e.g.*, apparatus vibrations, which are known to lead to a faster jet disintegration [10]. Indeed, a careful examination of the many other frames clearly shows that the nozzle executes vertical oscillations of amplitude $\lesssim 50 \mu\text{m}$. Since the individual frames are separated by time intervals of $1/16$ s it was not possible to determine the vibration frequency. A further occasional phenomenon caught by the camera contributes to confirm the above conclusion. Figure 2(c) shows a 2 mm long section of a continuous filament of solid $n\text{H}_2$ generated at $P_0 = 3$ bar and $T_0 = 17$ K, a configuration that would be invariably observed with the jet left undisturbed.

By comparing figs. 2(a) and (b), we deduce that jet freezing occurs at a distance between 0.2 mm and 0.4 mm from the nozzle exit. Freezing of the jet prior to Rayleigh breakup is not surprising and can be predicted on the basis of the theoretical analysis on the nucleation

process in molecular hydrogen [3]. The expected liquid filament temperature near the breakup point in fig. 2(b) is about 9 K. Since in earlier experiments on supercooling of hydrogen droplets the nucleation rate for $n\text{H}_2$ was measured to be a factor $\sim 10^3$ larger than for $p\text{H}_2$ [6], there follows $\Gamma(T \approx 9 \text{ K}) \approx 10^{16} \text{ cm}^{-3}\text{s}^{-1}$. Thus the *maximum* $n\text{H}_2$ liquid jet decay length can be estimated as $\ell + v/(4d_0^3\Gamma) \approx 0.4 \text{ mm}$, which is consistent with our experimental observations. Extrapolation of the present results to para-hydrogen leads us to conclude that the $p\text{H}_2$ microjet would invariably stay liquid until Rayleigh breakup occurs.

A well-suited technique for the experimental characterization of the actual liquid stream temperature is provided by Raman spectroscopy. Wilson *et al.* [23] were the first to successfully apply Raman spectroscopy for the determination of the bulk temperature in liquid water microjets under high-vacuum conditions. As demonstrated recently in seminal experiments on small $p\text{H}_2$ clusters it is the Raman shift of the Q -branch spectral feature that is a sensitive function of the liquid-hydrogen temperature [22].

Photons appear also to be the ideal atomic probe candidate to searching for the onset of superfluidity in liquid- $p\text{H}_2$ microjets. For example, quasi-elastic X-ray scattering experiments might be carried out to determine the static structure factor $S(Q)$ [24], which shows a loss of spatial order across the superfluid transition due to the condensation of atoms into a state of definite (zero) momentum [1]. Inelastic (Brillouin) light scattering is ideally suited for probing the hydrodynamic regime, *i.e.*, to study the behavior of the second sound component in the dynamic structure factor in the superfluid phase [25]. Low-frequency collective excitations along with their temperature dependence might be efficiently probed by Raman light scattering. A photon can create any two excitations, provided the net momentum is almost zero in order to compensate for the small change in the photon momentum. In this sense, Raman scattering in superfluid ^4He yielded impressive evidence for the existence of two-roton bound states [26]. The Raman shift is expected to be $\simeq 2\Delta$, where the roton energy gap in superfluid para-hydrogen has been estimated to be $\Delta \sim 10 \text{ K}$ [3].

In conclusion, we have presented a new approach for the experimental realization of a macroscopic sample of supercooled liquid molecular para-hydrogen at temperatures down to 1.3 K. As a critical step we demonstrated the feasibility to producing stable hydrogen microjets under vacuum conditions. This technique, specifically the unique possibility to control the sample temperature in a wide range across the predicted superfluid transition, coupled to light scattering experiments has the great potential to addressing the conjectured superfluidity in bulk liquid $p\text{H}_2$.

* * *

REG acknowledges support from GSI. We thank B. DOAK for many stimulating discussions and H. WUTTKE for assistance during nozzle preparation.

REFERENCES

- [1] TILLEY D. R. and TILLEY J., *Superfluidity and Superconductivity* (IOP Publishing, Bristol) 2001.
- [2] GINZBURG V. L. and SOBYANIN A. A., *JETP Lett.*, **15** (1972) 242.
- [3] MARIS H. J., SEIDEL G. M. and HUBER T. E., *J. Low Temp. Phys.*, **51** (1983) 471.
- [4] APENKO S. M., *Phys. Rev. B*, **60** (1999) 3052.
- [5] VOROBEV V. S. and MALYSHENKO S. P., *J. Phys. Condens. Matter*, **12** (2000) 5071.
- [6] MARIS H. J., SEIDEL G. M. and WILLIAMS F. I. B., *Phys. Rev. B*, **36** (1987) 6799.
- [7] TORII R. H., MARIS H. J. and SEIDEL G. M., *Phys. Rev. B*, **41** (1990) 7167.

- [8] SCHINDLER M., DERTINGER A., KONDO Y. and POBELL F., *Phys. Rev. B*, **53** (1996) 11451.
- [9] GREBENEV S., SARTAKOV B., TOENNIES J. P. and VILESOV A. F., *Science*, **289** (2000) 1532.
- [10] FROHN A. and ROTH N., *Dynamics of Droplets* (Springer, Berlin) 2000.
- [11] FAUBEL M., SCHLEMMER S. and TOENNIES J. P., *Z. Phys. D*, **10** (1988) 269.
- [12] FAUBEL M., in *Photoionization and Photodetachment*, edited by NG C. Y. (World Scientific, Singapore) 2000.
- [13] SMITH J. D., CAPP A C. D., WILSON K. R., MESSER B. M., COHEN R. C. and SAYKALLY R. J., *Science*, **306** (2004) 851.
- [14] BERGLUND M., RYMELL L., HERTZ H. M. and WILHEIN T., *Rev. Sci. Instrum.*, **69** (1998) 2361.
- [15] LORD RAYLEIGH, *Proc. R. Soc. London, Ser. A*, **29** (1879) 71.
- [16] GRISENTI R. E. and TOENNIES J. P., *Phys. Rev. Lett.*, **90** (2003) 234501.
- [17] KELLER W. E., *Helium-3 and Helium-4* (Plenum Press, New York) 1969.
- [18] At such low pressures the helium concentration in the liquid can be neglected; see, *e.g.*, STREETT W. B., SONNTAG R. E. and VAN WYLEN G. J., *J. Chem. Phys.*, **40** (1964) 1390.
- [19] RANZ W. E. and MARSHALL W. R., *Chem. Eng. Prog.*, **48** (1952) 141.
- [20] VERKIN B. I. *et al.*, *Handbook of Properties of Condensed Phases of Hydrogen and Oxygen*, edited by SELOVER T. B. jr. (Hemisphere Publishing Corporation, New York) 1991.
- [21] LEVI A. C. and MAZZARELLO R., *J. Low Temp. Phys.*, **122** (2001) 75.
- [22] TEJEDA G., FERNÁNDEZ J. M., MONTERO S., BLUME D. and TOENNIES J. P., *Phys. Rev. Lett.*, **92** (2004) 223401.
- [23] WILSON K. R., RUDE B. S., SMITH J., CAPP A C., CO D. T., SCHALLER R. D., LARSSON M., CATALANO T. and SAYKALLY R. J., *Rev. Sci. Instrum.*, **75** (2004) 725.
- [24] CUNSOLO A., PRATESI G., COLOGNESI D., VERBENI R., SAMPOLI M., SETTE F., RUOCCO G., SENESI R., KRISCH M. H. and NARDONE M., *J. Low Temp. Phys.*, **129** (2002) 117.
- [25] GREYTAK T. J., in *Quantum Liquids*, edited by RUVALDS J. and REGGE T. (North-Holland, Amsterdam) 1978.
- [26] GREYTAK T. J., WOERNER R., YAN J. and BENJAMIN R., *Phys. Rev. Lett.*, **25** (1970) 1547.